

Quantum tunneling and motional narrowing of HD NMR line shapes in solid hcp H₂

J. M. Delrieu and N. S. Sullivan

*Service de Physique du Solide et de Résonance Magnétique, Center d'Etudes Nucléaires, Saclay,
91191 Gif-sur-Yvette Cédex, France*

(Received 17 November 1980)

The observed narrowing of the NMR line shapes of HD impurities in solid parahydrogen is interpreted in terms of a motional narrowing effect due to quantum tunneling. This model is successful in describing the dependence of the HD linewidths on the orthohydrogen concentration (0.1–4 at.%) and predicts a tunneling frequency $J \sim 1$ kHz. This value can be understood in terms of current views of tunneling in quantum solids which predict that three-body cyclic permutations dominate the tunneling processes in hcp ³He and H₂. Estimates of the tunneling frequencies to be expected for H₂ based on the experimental values for ³He are in close agreement with those needed to explain the NMR results.

I. INTRODUCTION

Low-temperature NMR experiments^{1,2} on HD (400 ppm) and ortho-H₂ (0.1–4 at.%) impurities in solid para-H₂ have revealed the existence of a significant hitherto unsuspected movement of the molecules in solid hcp hydrogen at very low temperatures ($T \geq 25$ mK). The proton NMR line shapes of the HD impurities are apparently Lorentzian and have a temperature-independent linewidth at least an order of magnitude smaller than that calculated for a rigid lattice. This suggests that the HD line shape is narrowed by some mechanism which modulates the dipole-dipole interactions between the HD molecules and the ortho-H₂ molecules (the para-H₂ molecules with total nuclear spin $I=0$ do not contribute). Nevertheless, the linewidths of the signals attributed to *isolated* ortho-H₂ molecules¹ are not narrowed and any mechanism used to explain the motional narrowing of the HD spectra must be effectively quenched for the ortho-H₂ molecules.

These properties can be understood if one introduces a large three-body cyclic permutation rate for molecules in hcp hydrogen analogous to that predicted for hcp ³He.³ Early estimates of the tunneling (or exchange) rate in solid hydrogen based on two-particle exchange calculated using single-particle Gaussian wave functions and two-body Jastrow correlation functions lead to very small two-body exchange frequencies⁴ (10^{-4} to 10^{-1} Hz) which are at least three orders of magnitude too small to explain the NMR results. This method which considers only two-body correlations is, however, inadequate for the description of the correlations during the tunneling processes. The theory of tunneling in quantum crystals has to be reexamined in order to understand the origin of the preponderant four-body and three-body tunneling rates (with respect to two-body exchange)

needed to explain the unusual properties of solid ³He at temperatures where the exchange leads to nuclear spin ordering.^{5–8}

Delrieu, Roger, and Hetherington^{3,7,8} have made a first step in this direction by considering the restriction imposed by the hard-core repulsions on the “true” wave function during the tunneling. They show that the most significant type of tunneling is that which requires the least disturbance for the surrounding atoms. Four-particle permutations are favored for bcc ³He while three-particle permutations dominate the tunneling processes in hcp ³He. This means that the “exchange” frequencies deduced from NMR experiments in hcp ³He should be attributed principally to three-body cyclic permutations rather than two-body exchange. For example, we consider a box of hard spheres representing the atoms located at the sites of an hcp lattice; at high densities, when the box is small, no exchange of the spheres is allowed and on increasing the size of the box (thereby reducing the density) the first type of exchange that is allowed is a three-body cyclic permutation. (The reader is referred to Ref. 3 for a comprehensive discussion.)

In Sec. II we present two methods for the estimation of the permutation frequency in solid para-H₂ using the simple model of Delrieu *et al.*^{3,7,8} We show that solid H₂ is similar to solid ³He at a density of 15 cm³/mol. This model fits quantitatively the observed frequencies in solid hcp ³He as a function of the density and we use it to calculate the tunneling frequency in solid H₂. The essential point is that the Gaussian overlap formula for the exchange used by Oyarzun and Van Kranendonk⁴ must be replaced by a formula for the tunneling frequency which is exponential and not Gaussian. The physics of the tunneling processes in the model presented below is particularly transparent and we limit the analysis to a

simple formulation.

In Sec. III we discuss the physical consequences for the experimental results and in particular explain why HD impurities undergo fast movement contrary to ortho-H₂ impurities for which interchange is inhibited by their large mutual quadrupolar interactions. Finally, we present additional physical consequences of the tunneling motion which remain to be tested.

II. CALCULATION OF THE TUNNELING FREQUENCIES

A. Previous calculations

Oyarzun and Van Kranendonk⁴ have estimated the exchange frequency in solid hydrogen by using the simple formula obtained by Guyer and Zane⁹ from the overlap of single-particle Gaussian wave functions

$$J = \frac{3}{5} (2\pi)^{-1/2} \frac{\hbar \alpha^2}{m} \alpha^3 \sigma^2 R_0 \exp\left[-\frac{1}{2} \alpha^2 (R_0^2 + \sigma^2)\right], \quad (1)$$

σ is the Lennard-Jones diameter, R_0 the lattice constant, m the molecular mass, and α the width of the single-particle distribution. They find for H₂ at $P=0$, $J \sim 10^{-4}-10^{-1}$ Hz. It is instructive to observe to what extent the values of J given by formula (1) fit the experimental values for the exchange in solid ³He. The calculated value of J is extremely sensitive to the exact value of α^2 in the exponential but the values of α^2 reported in the literature are unfortunately inconsistent. Guyer and Zane⁹ find values of J three times smaller than the experimental ones using the values of α^2 given by Sarkissian¹⁰ and it has been shown by Mac Mahan¹¹ that α^2 remains essentially undetermined to within a factor of 2. The most reliable value of α^2 seems to be that obtained by Hansen and Levesque¹² who use an exact Monte Carlo integration of the variational wave function to calculate the ground-state energy. They find values of

α^2 smaller than those quoted by Sarkissian¹⁰ (by approximately 2) and for Hansen and Levesque's values we calculate using formula (1), exchange frequencies $J \sim 5$ GHz for $V_m = 24$ cm³/mol and $J \sim 200$ MHz for $V_m = 18$ cm³/mol for solid ³He. These theoretical values are 300 times larger than the experimental values.

In a revised calculation Landesman⁹ finds a different preexponential factor for formula (1) which reduces the calculated values of J by a factor of approximately 10. Since the values of α^2 are significantly larger for solid H₂, it is clear that we cannot have any confidence in the crude formula (1) for the exchange frequency. The most compelling reason for reanalyzing the calculation of tunneling frequencies in quantum solids is the need to understand the origin of the three- and four-particle exchange needed to explain the low-temperature properties of solid ³He.

B. Similarities between the tunneling in solid H₂ and solid ³He

The first obvious approach is to use the experimental tunneling frequency for solid ³He as a scale to estimate the frequency in solid H₂. We first consider the difference in the interaction potentials for H₂ and ³He. Both are essentially hard-core potentials with a small long-range attractive contribution (see review paper of Silvera¹³). It is interesting to normalize these potentials $U(r)$ to their hard-core diameter a using reduced units r/a and $(U)2m\sigma^2/\hbar^2$. The value of the hard-core diameter is given by Kalos *et al.*¹⁴ as the scattering length of the repulsive hard-core contribution to the potential, $a = 0.8368\sigma$, where σ is the characteristic length of the Lennard-Jones potential [$U(\sigma) = 0$]. The values of these parameters for H₂ and ³He are listed in Table I and the normalized potentials are compared in Fig. 1. The potential for H₂ is deeper than that for ³He resulting in a shorter equilibrium distance r_{eq} (in reduced units) for H₂. The value of r_{eq} for H₂ at $V_m = 22.8$ cm³/mol

TABLE I. Parameters used in the calculation of the tunneling frequencies in hcp ³He, hcp H₂, and hcp D₂. R_m and ϵ_m define the minima of the pair potentials of Fig. 1 in reduced units. $a = 0.8368\sigma$ is the hard-core diameter (Ref. 14). The compressibilities are taken from the experimental results given in Refs. 20 and 13.

	V_m (cm ³ /mol)	R_0 (Å)	σ (Å)	a (Å)	R_m	ϵ_m	P (bar)	β (10 ⁻³ bar ⁻¹)	J (μK)	J (kHz)
³ He	19.25	3.56	2.556	2.319	1.34	8.32	118	1.64	14.4	300
	18.0	3.48	2.556	2.319	1.34	8.32	171	1.04	1.28	27
	17.75	3.47	2.556	2.319	1.34	8.32	188	1.00	0.88	18
H ₂ (para)	23.16	3.79	2.96	2.477	1.42	24.95	0	0.48	0.46	9.5
	22.0	3.72	2.96	2.477	1.42	24.95	110	0.36	0.006	0.12
D ₂ (ortho)	19.95	3.61	2.96	2.477	1.42	24.95	0	0.25	10 ⁻⁶	~10 ⁻⁵

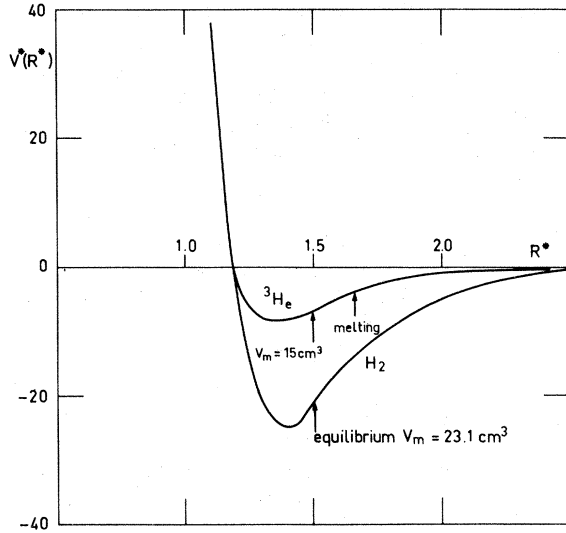


FIG. 1. Pair potentials for ${}^3\text{He}$ and H_2 in reduced units $V^*(R^*) = V(R)/(\hbar^2/2m\sigma^2)$ and $R^* = R/a$ where σ is the characteristic length of the Lennard-Jones potential [$V^{LJ}(\sigma) = 0$] and $a = 0.8368\sigma$ is the hard-core diameter (Ref. 14). The ${}^3\text{He}$ - ${}^3\text{He}$ potential is calculated for a Lennard-Jones form ($V_{\min} = -10.22$ K, $\sigma = 2.556$ Å) and the H_2 - H_2 potential is taken from the semiempirical form discussed by Silvera (Ref. 13) ($V_{\min} = -34.3$ K, $\sigma = 2.96$ Å). The distances corresponding to the nearest-neighbor lattice spacings are indicated by the arrows in the figure.

corresponds to reduced units to solid ${}^3\text{He}$ at a density of

$$V_m(\text{H}_2) \left(\frac{a({}^3\text{He})}{a(\text{H}_2)} \right)^3 = 15.1$$

in cm^3/mol . As first pointed out by Kalos *et al.*,¹⁴ when $r_{\text{eq}} > r_m$ [where r_m is the distance for which $U(r)$ passes through a minimum], i.e., when the zero-point motional energy remains comparable to the potential energy, the wave function for quantum hard-core solids is very close to that of a hard sphere quantum solid. In this case the total energy is given by zero-order perturbation theory using the exact wave function of the hard sphere quantum solid. For this reason the wave functions of solid H_2 and solid ${}^3\text{He}$ at the same reduced volume are quite similar and their tunneling frequencies are therefore of the same order of magnitude in reduced units

$$J(\text{H}_2) \frac{2m_2\sigma_2^2}{\hbar^2} \approx J({}^3\text{He}) \frac{2m_3\sigma_3^2}{\hbar^2} \quad (2)$$

An extrapolation of the experimental values of J for hcp solid ${}^3\text{He}$ given in Fig. 32 of Ref. 15 for $15 < V_m < 17$ cm^3/mol gives $J(\text{H}_2) \approx 2$ kHz. This result is at least four orders of magnitude larger than that given by Oyarzun and Van Kranendonk.⁴

C. Model calculation of the tunneling in hcp ${}^3\text{He}$ and hcp H_2

A second method is to consider the physics of tunneling in solid ${}^3\text{He}$, in order to derive a simple expression fitting the experimental values in hcp ${}^3\text{He}$, which is then used to calculate the tunneling frequency in solid H_2 . This enables one to estimate the difference in the tunneling frequency for H_2 and ${}^3\text{He}$ at the same reduced molar volume V_m due to the differences in the attractive potentials. At first sight, since the potential decreases more for H_2 than for ${}^3\text{He}$ when the particles are close together, one would predict qualitatively that the tunneling frequency for H_2 is larger than that given by relation (2).

We will use the model presented in Ref. 3 based on the remarks of Thouless.¹⁶ The atoms spend most of their time near a given lattice site, i.e., in a configuration where the wave function ψ is maximum. Following Thouless we call this configuration a cavity. There are $N!$ possible permutations of the N atoms among the different lattice sites, and consequently there are $N!$ cavities in configuration space for the positions of the atoms. Exchange of some of the atoms then corresponds to a permutation movement of the atoms connecting two cavities via configurations of low probability since (as shown in Fig. 2) the hard-core repulsions severely reduce the available free space during exchange. In configuration space the tunneling is therefore described by a movement in a long narrow duct connecting two cavities. It is important to realize as stressed in Ref. 15, that the mathematical structure of the variational wave function (i.e., Gaussian) which is valid *inside* the cavities for the evaluation of the energy can be quite wrong for the description of the tunneling in the duct. For example, in a narrow duct of constant cross section, the wave function decreases exponentially along the duct in contradiction to the extrapolation of the Gaussian wave function. This explains clearly why the tunneling frequency can be severely underestimated using the formula (1) at high densities.

What is remarkable is the fact that in this duct, the pure potential energy U^P alone is reduced with respect to that in the cavities since during the tunneling, the particles are closer together (but remain at distances larger than r_m , except at very high densities) and therefore see a deeper potential during the exchange. The exchange in quantum solids should not therefore be regarded as a tunneling through a potential energy barrier but rather as a tunneling through a kinetic energy barrier U^Z associated with the reduced available zero-point motion for the exchanging particles (Fig. 2). The preceding estimate (Sec. II B) of J in H_2 starting from the experimental values for ${}^3\text{He}$ therefore neglects the difference in the potential energy δU^P for ${}^3\text{He}$ and H_2 with respect

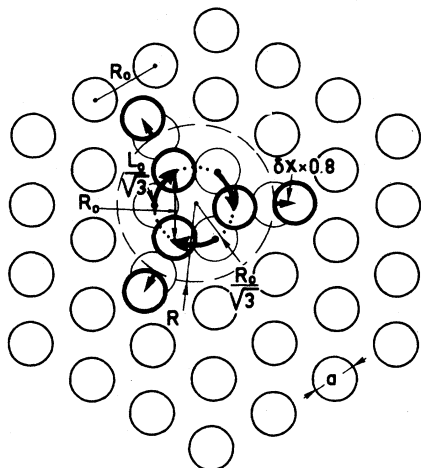


FIG. 2. Geometrical representation of three-particle tunneling (via cyclic permutation) in the (100) plane of an hcp lattice at the density of solid hydrogen ($R_0/a \approx 1.5$ where a is the hard-core diameter). The permuting atoms are the three atoms in the center which are maintained at the equilibrium distance R_0 from each other. They turn on a circle of radius $(1/\sqrt{3})R_0$. The three surrounding bold faced atoms move a distance $\delta x = (1 - 1/\sqrt{3})R_0$ if they are maintained at the distance R_0 from the exchanging atoms. In order to take into account the compressibility of these surrounding atoms, this displacement is reduced to $0.8\delta x$ in the figure. The volume taken by the three exchanging atoms is that of a cylinder of radius $R = (\frac{1}{2} + 1/\sqrt{3})R_0$ and of height $h_0 = \sqrt{2/3}R_0$ containing the three exchanging atoms (in the dashed circle of radius R). [When the upper (or lower) (100) plane has an atom above (or below) the center of the ring of exchanging atoms the upper and lower atoms are not perturbed in the exchanging configuration so that the equilibrium height h_0 is taken for the height of the cylinder.]

to that for the kinetic energy δU^2 during the exchange. This leads to errors since U^P and U^2 are of the same order of magnitude.¹⁷ For this reason a more detailed model is necessary.

It has been shown^{3,5,7,8} that the true wave function along a fall line $\mathcal{L}(t)$ in the duct obeys a one-dimensional Schrödinger equation

$$-\frac{\hbar^2}{2m} \frac{\partial^2 \psi}{\partial t^2} + V(t)\psi = E\psi, \quad (3)$$

where the effective potential

$$V(t) = -\frac{\hbar^2}{2m} \nabla_{\perp}^2 \ln \psi(t) + U;$$

∇_{\perp} is the gradient in configuration space orthogonal to the tangent to the line $\mathcal{L}(t)$, t being the curvilinear coordinate along the fall line. $V(t)$ can be evaluated using a variational function ψ in the place of ψ , because V is essentially the energy of the system in the exchange configuration for a given value of t . A complete consistent treatment of the problem is com-

plex because one would need to (i) evaluate $V(t)$ variationally and (ii) determine the optimum trajectory $\mathcal{L}(t)$ for the tunneling; i.e., the "most probable escape path" (MPEP)¹⁸ defined by the maximum value of ψ on the exchange surface Σ midway between the cavities. The MPEP corresponds to the trajectory which minimizes $\int \sqrt{2m(V-E)} dt$. It can be shown⁸ that this corresponds to a displacement of the surrounding atoms similar to that for a static elastic deformation for short distances with an exponential cutoff at long distances, in order to minimize the product $\sqrt{V}L$. [V is the effective potential related to this deformation and L the length of the line $\mathcal{L}(t)$.]

Although the solution of this complex problem is possible,⁸ it has not been pursued and we therefore consider a simple physical estimate of V and L . The tunneling frequency is then given by the difference in energy of the symmetrical and antisymmetrical eigenstates of the one-dimensional Schrödinger equation, Eq. (3). As shown in the thesis of Roger,¹⁸ the effective potential has an approximately sinusoidal shape as reproduced in Fig. 3. For this reason we take the simple shape with only one Fourier component.

$$V(t) = -\frac{\delta U}{2} \cos \frac{\pi t}{L} + \bar{V}, \quad (4)$$

which when used with Eq. (3) leads to a second-order differential equation which turns out to be Mathieu's equation¹⁹

$$\frac{d^2 y}{dv^2} + (a - 2q \cos 2v)y = 0 \quad (5)$$

for the variables $v = \pi t/2L$ and $q = -2mL^2 \delta U / \pi^2 \hbar^2$. The solutions b_1 and a_0 of Mathieu's equation as given by formula (20.2.31) of Abramowitz and

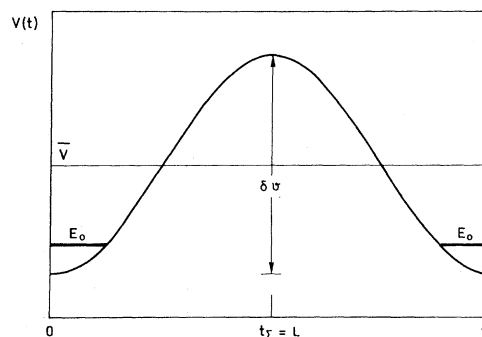


FIG. 3. Approximate form for the potential for the tunneling as a function of the distance t in configuration space. The point $t = t_{\Sigma}$ corresponds to the configuration shown in Fig. 2 for which the permuting particles are in positions of closest approach to their neighbors. (This corresponds to the center of the duct connecting the two cavities in configuration space.)

Stegun¹⁹ give the exchange frequency

$$\begin{aligned} 2hJ &= E_A - E_S \\ &= \frac{\hbar^2}{2m} \left(\frac{\pi}{2L} \right)^2 (b_1 - a_0) \\ &= 2^5 \left(\frac{2}{\pi} \right)^{1/2} \frac{\hbar^2}{2m} \frac{\pi^2}{4L^2} q^{3/4} e^{-4\sqrt{q}} \end{aligned} \quad (6)$$

For the J defined here the tunneling Hamiltonian becomes $H = J \sum \mathcal{O}_{ijk}$ where \mathcal{O}_{ijk} is the corresponding permutation operator. For a given tunneling process, J can be calculated once δU and L have been evaluated.

A simple valid estimate of the effective potential energy can be obtained by observing that the exchanging particles compress their surroundings and δv can therefore be taken to be the energy of compression of the surrounding particles due to the increase in volume ΔV taken by the exchanging particles

$$\delta U = \int_{V_0}^V P dV = -P \Delta V + \frac{1}{2\beta} \frac{(\Delta V)^2}{V_0} ; \quad (7)$$

$\Delta V = V - V_0$ is the increase in volume of the exchanging atoms, P the pressure, and $\beta = -(1/V) \partial V / \partial P$ the experimental compressibility at equilibrium at $T=0$. The tunneling is maximum for minimum ΔV (for a given length L) and the geometrical analysis of Ref. 3 shows that this corresponds to the cyclic permutation of three atoms as shown in Fig. 2. It should be noted that different types of three atom cyclic permutations can occur for an hcp configuration according to the different possible arrangements of the nearest neighbors of the exchanging atoms. For example, in Fig. 2, the upper (and lower) plane may, or may not, have an atom located at the center of the circle of the three permuting atoms. The same remark is true for the cyclic exchange of three atoms in planes other than the basal plane.

At equilibrium the volume V_0 of the three exchanging atoms is

$$V_0 = \frac{3}{\sqrt{2}} R_0^3 = 3V_m \quad (8)$$

for the hcp lattice. (R_0 is the nearest-neighbor separation.) In the exchanging configuration, the volume taken by the exchanging atoms (taken to be at a separation R_0) is that of a cylinder of height

$$h_0 = \sqrt{2/3} R_0 \quad (9)$$

(equal to the height of the cylinder occupied by each atom in equilibrium) and radius

$$R = \left(\frac{1}{2} + \frac{1}{\sqrt{3}} \right) R_0 \quad (10)$$

as shown in Fig. 2; R is the radius of the circle drawn through the center of the three-nearest surrounding atoms at their equilibrium position. The increase in volume is therefore

$$\Delta V = V - V_0 = \pi R^2 h_0 - V_0 = 1.21 V_m \quad (11)$$

The exchange length $L = [\sum_i (\delta x_i)^2]^{1/2}$ is given by the sum of the squares of displacements of (i) the three exchanging atoms, each of which moves on a circle of radius $R - \frac{1}{2} R_0 = R_0/\sqrt{3}$ with an angular displacement $\pi/3$, giving

$$L_0 = \left[3 \left(\frac{\pi R_0}{3\sqrt{3}} \right)^2 \right]^{1/2} = \frac{\pi}{3} R_0 \quad (12)$$

and (ii) the displacement of the surrounding atoms which is essentially that of the three neighboring atoms as shown in Fig. 2. If the latter are maintained at a distance R_0 from the other atoms, they move a distance

$$\delta x = \left[1 - \frac{1}{\sqrt{3}} \right] R_0 \quad (13)$$

In order to take into account the compressibility of the surroundings we reduce this displacement to $0.8\delta x$. Only a detailed complex solution of the displacement of the atoms in the potential V could give an exact description of the compression of the surrounding atoms, and also of the exchanging atoms. Nevertheless, this simplified estimate will not be far from the true value. Thus we take

$$L = [L_0^2 + 3(0.8\delta x)^2]^{1/2} = 1.2R_0 \quad (14)$$

Using the experimental values of the compressibility given by Straty and Adams²⁰ (see Table II), the theoretical values of the three-particle cyclic permutation (or exchange) frequency can be calculated for solid ³He using formulas (5), (6), (7), (8), (11), and (14). The results of the calculation are shown in Fig. 4 as a function of the molar volume and compared with the experimental values given by Guyer, Richardson, and Zane.¹⁵ The agreement is satisfactory. We have also used this formula for the bcc phase of solid ³He although the nature of the exchange is in this case physically different and corresponds to multiple four-spin exchange for which formula (6) is valid if we know the values of ΔV and L . For the bcc phase we therefore have an equivalent empirical formula for ΔV and L , and the close fit to the experimental data shows that ΔV and L are of the same order of magnitude in the hcp and bcc phases at the equivalent densities, although the nature of the exchange is different for the two phases.

Since the tunneling frequencies calculated using the model described above are in good agreement with those determined experimentally for hcp ³He for a wide range of densities, we can confidently apply the

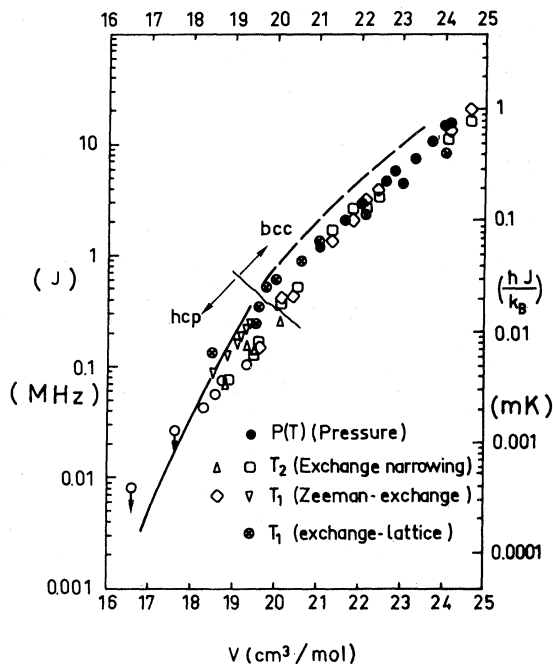


FIG. 4. Comparison of the calculated tunneling frequencies and the experimental values for ^3He as deduced from heat-capacity measurements and NMR experiments (see Ref. 15). The solid line represents the frequencies calculated from Eq. (16) in the text using experimental values of the compressibility β for the different molar volumes of hcp ^3He . The broken line gives the values obtained from the same formula using experimental values of β for the bcc phase of ^3He at different densities. Formula (6) in the text is of course applicable for both three and four atom tunneling provided one uses the correct volume change and path length for the permuting atoms. (All the high-temperature NMR results have up until now been interpreted in terms of a Heisenberg exchange interaction.) In the hcp phase the predominant three-atom tunneling can be expressed as a sum of three Heisenberg interactions and the values of J cited in Ref. 15 are directly related to the three-atom tunneling rate. While both four-atom and three-atom exchange predominate in the bcc phase, thereby complicating the analysis of the NMR results, the values of J cited in the literature do nevertheless provide an estimate of the three-atom and four-atom tunneling rates (Ref. 8).

same formula (6) to hcp H_2 using the compressibility data published by Wanner and Meyer²¹ (see Table I). We find $J \approx 9$ kHz at $P=0$ and $J \approx 130$ Hz at $P=100$ bars. This shows that the tunneling frequency in solid H_2 is also a very sensitive function of the pressure as a result of the rapid decrease of the compressibility with increasing density.¹³

This new physical model of the exchange relates the tunneling frequency to the elastic properties of the solid. The experiments of Refs. 1 and 2 were sensitive to the movement of HD impurities in hcp H_2 . We therefore need to estimate the cyclic permu-

tation frequency of one HD molecule with two para- H_2 molecules. The potential U between the HD molecule and a para- H_2 molecule is the same as that between two para- H_2 molecules. Nevertheless, the mass of the HD molecule is 3 compared to the mass 2 of the H_2 molecule and this leads to two opposing effects for the *effective* potential δU in expression (4). Firstly, at equilibrium, the zero-point motional deviation of an HD molecule is reduced by a factor of $\sqrt{2/3}$ with respect to that of H_2 , so that the surrounding para- H_2 molecules around an HD impurity have more available space for their own zero-point motion. For this reason, the compressibility of the para- H_2 around an HD impurity is larger than that of pure para- H_2 and δU is therefore expected to decrease slightly. Secondly, the increased mass of HD is equivalent to an increase in the path length L for the exchange, each displacement being weighted by the mass of the corresponding atom in Schrödinger's equation. The total mass of the exchanging particles (two para- H_2 and one HD molecule) is 7 in contrast to the value 6 for pure para- H_2 . The length L is therefore increased by a factor $\sqrt{7/6}$. The value of $q \propto \delta U L^2$ entering in the calculation of the tunneling frequency therefore changes only slightly for HD impurities due to the opposing variation of L and δU . In the context of this model which explains quantitatively the observed exchange in hcp ^3He we expect a significant three-body tunneling frequency of the order of 1 kHz for HD impurities in para- H_2 .

We will now consider the physical consequences of this model for the tunneling in solid H_2 for the NMR properties of HD and ortho- H_2 impurities. In view of the complexity of the interactions between the different types of impurities we will limit ourselves to a simple physical description of the essential features, leaving a large number of unsolved problems.

III. DISCUSSION OF THE NMR RESULTS

The rapid tunneling in hcp H_2 predicted by the above arguments leads to a delocalization of the HD and ortho- H_2 impurities if the interactions between the impurities are negligible. These impurities then behave as quasiparticles²² (wavelike excitations) that migrate freely through the crystal with constant group velocity. The NMR properties of these impurities in para- H_2 (linewidth, spin diffusion, relaxation, etc.) are therefore to be closely related to those observed for ^3He impurities in ^4He .²³⁻²⁹ We therefore expect a substantial motional narrowing³⁰ of the HD line shape due to the modulation of the dipole-dipole interactions between the HD molecules and the ortho- H_2 molecules. In order to estimate the NMR linewidth of the HD or ortho- H_2 molecules we need to consider how the motion of these impurities is affected by their mutual interactions. We consider

firstly the motion of the ortho-H₂ molecules and secondly that of HD impurities.

As pointed out by Oyarzun and Van Kranendonk⁴ it is important to note that the tunneling of the ortho-H₂ molecules is severely reduced by their relatively large quadrupole-quadrupole interactions

$$V_{QQ} \approx \Gamma(R_0/R)^5,$$

with

$$\Gamma \approx 0.8 \text{ K},$$

which leads to a band of energies of half-width $\hbar\omega_Q = 20\Gamma X^{5/3}$,^{31,32} where X is the ortho-H₂ concentration. This value for $\hbar\omega_Q$ is consistent with the NMR experiments of Buzerak *et al.*³² After tunneling from one site to a neighboring site, the energies of the initial and final states of the ortho-H₂ molecules differ by

$$\hbar\omega_Q \gg hJ \quad (J \approx 10^4 \text{ Hz})$$

and only a fraction

$$\frac{2\pi J}{\omega_Q} \approx 2 \times 10^{-7} X^{-5/3}$$

of all possible transitions can conserve energy. The effective tunneling frequency of the ortho-H₂ molecules is therefore reduced to 2.10^{-3} Hz for $X \approx 1$ and the line shape of the isolated ortho-H₂ molecules retains its rigid lattice linewidth. It is interesting to note that for very low ortho-H₂ concentrations, the tunneling frequency is no longer blocked and one expects a motional narrowing of the ortho-H₂ line shape for ortho concentrations.

$$X < X_{CR} \approx \left(\frac{2\pi J}{\omega_Q} \right)^{3/5} \lesssim 0.01\%.$$

For ortho concentrations X greater than X_{CR} we therefore consider the ortho-H₂ molecules as remaining fixed.

We now consider how the interactions between the static ortho-H₂ impurities and the mobile HD impurities affect the motion of the HD molecules. For the experiments discussed in Refs. 1 and 2, the ortho-H₂ concentrations (0.1–4 at. %) are much higher than the HD concentrations (400 ppm) and the contribution of the HD-HD dipolar interactions to the HD linewidth can be neglected. Unlike the ortho-H₂ molecules, the HD molecules are in an orbital quantum state $\mathcal{J}=0$. They have no orientational degree of freedom, and we can treat them as spherical defects.

Each HD impurity creates a lattice deformation in its neighborhood due to the difference in the zero-point motion of the impurity compared to that of the host para-H₂ molecules. This elastic deformation sets up an anisotropic interaction between the HD and the

ortho-H₂ impurities. The strain surrounding an HD molecule is due to the difference between the zero-point translational motion of the HD molecule and the lighter para-H₂ molecules. This creates a long range $1/R^3$ elastic strain field in the crystal analogous to that estimated for ³He impurities in hcp ⁴He.³³ The origin of the deformation surrounding an ortho-H₂ impurity is quite different. In this case the mass of the ortho-H₂ molecules and the para-H₂ molecules is identical and the strain field results from the coupling of the rotational degrees of freedom of the ortho-H₂ molecule with the translational degrees of freedom. In an otherwise pure para-H₂ crystal isolated ortho-H₂ molecules experience a crystal field.^{34,35}

$$V_i = \sum_j B(R_{ij})(1 - 3 \cos^2 \theta_{ij}),$$

where $B(R)$ contains a short-range repulsive term and a relatively long-range attractive term $\alpha(R_0/R)^6$ (Refs. 34 and 35). For an hcp lattice the lattice sum \sum_j is vanishingly small and the observed crystal field³⁶ $V_c \approx 10$ mK is due to the weak dependence of $B(R)$ on the angular momentum ($\mathcal{J}=1$) of the ortho molecule and deviations from ideal hcp packing. The crystal fields quoted in the literature^{32,33} refer in general to the separation of the lowest energy levels $\mathcal{J}_z=0$ from the degenerate levels $\mathcal{J}_z = \pm 1$. While this describes the energies of the *orientational* configurations of the ortho molecules with respect to the local crystal molecules it must be remembered that the crystal-field interactions lead to *two* effects: (i) the lifting of the degeneracy of \mathcal{J}_z levels (i.e., the orientational crystal field) and (ii) an isotropic lowering of the center of gravity of the \mathcal{J}_z levels with respect to the energy of the unperturbed ortho-H₂ molecule. These two effects are comparable³⁵ and both must be considered in estimating the interaction between the ortho-H₂ and the HD molecules. If the isotropic crystal fields of the ortho-H₂ impurities were considered separately one would expect a long-range interaction between the HD and ortho-H₂ impurities of the form

$$U'(R_{12}) = U'_0 (R_0/R_{12})^3 F'(\theta_{12})$$

analogous to that estimated for ³He impurities in ⁴He.³⁷ R_{12} is the separation of the impurities and $F(\theta_{12})$ is an angular factor depending on the anisotropy of the elastic force constants of the host crystal. The anisotropic coupling of the ortho-H₂ molecules to the lattice would lead to a shorter-ranged interaction

$$U''(R_{12}) = U''_0 (R_0/R_{12})^7 F''(\theta_{12}).$$

In view of the complexity of this problem we have not attempted any calculation of U'_0 or U''_0 for H₂ and we will consider only a generalized interaction of

the form

$$U(R_{12}) = U_0(R_0/R_{12})^n F(\theta_{12}) \quad (15)$$

The kinetic energy of an HD impurity is $\sim \hbar J$ and it can approach an ortho-H₂ molecule to within a distance R_c such that $U(R_c) \approx J$

$$R_c = R_0(U_0/J)^{1/n} \quad (16)$$

If the mean separation of the impurities $\bar{R} = X^{-1/3}R_0 \gg R_c$, the HD impurities can be regarded as a rarefied gas of quasiparticles or impuritons²²⁻²⁵ having states of well-defined energy and momentum. (Energy bandwidth $\sim \hbar J$, group velocity $v_g = \partial E/\partial p \approx JR_0$.²²) The diffusion of the HD impuritons can therefore be treated using ordinary gas-kinetic theory. The diffusion constant $D = v_g \lambda$ where the mean free path

$$\lambda = 1/(n\sigma) = R_0^3/(\sigma X) \quad , \quad \sigma = \pi R_c^2$$

is the cross section for the impuriton scattering in the crystal field due to fixed ortho-H₂ impurities of concentration X .

This impuriton gas regime is valid for very low ortho concentrations $X \ll X_c$ where

$$X_c = (J/U_0)^{3/n} \quad (17)$$

is the concentration for which the mean separation \bar{R} becomes equal to the distance R_c for which the kinetic energy is comparable to the elastic interactions. For high concentrations $X \gg X_c$, the motion of the HD impurities is completely modified. As a result of the elastic interactions the HD molecules are in strong continuous interactions with the ortho-H₂ impurities, the motion is no longer coherent but can be described by a diffusive motion²² with $D_{SI} = v_g^2 \tau_D$ where

$$\tau_D = \frac{\hbar}{|a \nabla U|} = \hbar X^{-(n+1)/3}/U_0 \quad (18)$$

Having established the nature of the movement of the HD impurities as modified by the crystal-field interactions we are now in a position to estimate the transverse NMR relaxation rates.

A. Impuriton regime $X \ll X_c$

In this regime the HD impurities travel freely through the crystal until they are scattered by the ortho-H₂ impurities. The proton spin of the HD molecule sees a rapidly changing local magnetic field for a short time t_d of the order of the duration of the collision with the ortho-H₂ impurities. The local field seen by the HD molecules consists of sharp spikes lasting for a time $t_d = R_c/v_g$, but for all practical purposes constant between collisions. The amplitude of

the modulation of the local field during the collision is $\Delta H_d = (\gamma \hbar/R_c^3)$. For the diffusive motion described above the collisions occur at a frequency $\tau_{\text{coll}}^{-1} = v_g^2/D$ and the transverse NMR relaxation rate is given by²⁴

$$\begin{aligned} \frac{1}{T_2} &= \langle (\gamma \Delta H_d t_d)^2 \rangle \tau_{\text{coll}}^{-1} \\ &= \frac{M_{2r}}{J} \left(\frac{R_0}{R_c} \right)^2 \end{aligned}$$

$M_{2r} = 67X \text{ kHz}^2$ is the rigid lattice second moment for the HD-ortho-H₂ nuclear dipole-dipole interactions. Using the expressions (16) and (17) for the concentration X_c for which the impuriton gas regime crosses over to the continuous interaction regime, we have $(R_c/R_0) = X_c^{-1/3}$ for all values of n and the relaxation rate can be written as

$$\frac{1}{T_2} = M_{2r}(X)/J_{\text{eff}} \quad (19)$$

where

$$J_{\text{eff}} = JX_c^{-2/3} \quad (20)$$

The HD linewidth $\Delta \approx 1/T_2$ depends linearly on the concentration for $X < X_c$ and this is certainly consistent with the experimental results of Constable² shown in Fig. 5. The solid line for the impuriton gas regime fits the data for $J_{\text{eff}} = 5.6 \text{ kHz}$. Although there are insufficient results for a reliable determination of X_c the results plotted in Fig. 5 indicate an onset of the continuous interaction regime for $X_c \approx 3$ at.%. Using this value we find from Eq. (20) a tunneling frequency $J \approx 0.6 \text{ kHz}$ which is in good agreement with the above estimates. Some care has to be taken when comparing these results to the rigid lattice linewidth to be expected in the absence of motional narrowing. For the range of ortho-H₂ concentrations we are considering, the rigid lattice line shape is expected to change from approximately Gaussian shape with rms width (in kHz)

$$\Delta_G(X) = M_{2r}^{1/2}(X) = 8.2X^{1/2} \quad ,$$

for $X > 1$ at.% to a Lorentzian shape for low X whose half intensity width is much smaller than the rms width. In the limit $X \ll 1$ at.% a statistical calculation of the width becomes appropriate³⁸ and for spin-one particles we find

$$\Delta_S = 10.1\gamma^2 \hbar n = 33X \text{ kHz}$$

(n is the density of ortho-H₂ molecules). In the intermediate concentration range ($X \sim 1$ at.%) the observed NMR linewidths of dilute ortho-H₂ samples ($1.5 < X < 2.5$ at.%)³⁹ and ²⁹Si (4.7 at.% abundance)⁴⁰ are approximately a factor of 2 higher than those calculated using the statistical theory. For dilute ortho-H₂, Pedroni *et al.*³⁹ observe a half intensity

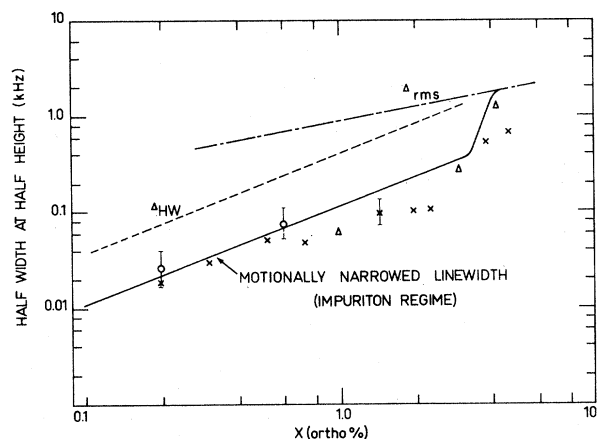


FIG. 5. Variation of the HD NMR linewidth in solid hcp hydrogen as a function of the orthohydrogen concentration. The solid line represents the best fit to the data assuming a tunneling frequency $J = 5.6$ kHz. The crossover in the concentration dependence at $X_c \approx 2$ at. % is interpreted in terms of a change in regime for the motion of the HD impurities: free coherent gaslike propagation for $X < X_c$, as opposed to a constant interaction regime for $X > X_c$ when the mean HD-ortho- H_2 separation becomes comparable to the range of their interaction. The triangles refer to the data of Schweizer *et al.* (Ref. 1) obtained at 25 mK and the open circles to the data of Constable (Ref. 2) for $33 < T < 80$ mK. (For low temperatures $T \leq 50$ mK and low ortho concentrations $X < 1$ at. %, both groups report essentially temperature-independent Lorentzian line shapes.) The broken line represents the rigid lattice rms width $\Delta_{rms} \approx 8.2X^{1/2}$ kHz which gives the half-width for $X > 1$ at. %, and the dashed line represents the estimated rigid lattice half-width $\Delta_{HW} \approx 35X$ kHz for $X < 1$ at. % using the results of Pedroni *et al.* (Ref. 39). (See Ref. 40a.)

width (in kHz)

$$\Delta_{rigid}^{expl}(X) \approx 70X$$

for $X \approx 1$ at. % and we take this value as a realistic estimate of the rigid lattice linewidth in the intermediate concentration range. This is given by the dashed line in Fig. 5.

B. Continuous interaction regime

Although the motion of the HD molecules is no longer coherent it can be described in terms of a diffusion $D_{SI} = v_g^2 \tau D$ [Eq. (18)]. The spin-spin relaxation is dominated by the rapid change in the local field $\Delta H'_d \approx (\gamma \hbar / R_0^3)$ which occurs when an HD molecule diffuses to within a lattice spacing R_0 of an ortho- H_2 molecule. This lasts for a time $t'_d \approx a/v_g$ and the transverse relaxation rate

$$\frac{1}{T_2} = M_{2r}(X)^{(n-2)/3} / J'_{eff} ,$$

where

$$J'_{eff} = J^2 / U_0 .$$

[The term $X^{(n-2)/3}$ becomes $X^{1/3}$ for the cubic interaction $U \propto U_0 (R_0/R)^3$ which is believed to be dominant for ^3He impurities in solid ^4He .^{37]}

The experimental results shown in Fig. 5 for $X > X_c \approx 3\%$ would seem to indicate a much stronger concentration dependence than the $X^{4/3}$ dependence predicted for ^3He impurities in solid ^4He . The broken line shown in Fig. 5 is for an $X^{7/3}$ dependence as expected for a $1/R^6$ interaction. One should note that the apparently well-defined distinction of the linewidth $\Delta(X)$ shown in Fig. 5 can be used to obtain three pieces of information: (i) $JX^{-2/3}$ from the slope of $\Delta(X)$ for $X \ll X_c$, (ii) $X_c = (J/U_0)^{3/n}$ from the transition between the two regimes, and (iii) the exponent n from the slope $X^{(n+1)/3}$ for $\Delta(X)$ for $X > X_c$. These results allow us to infer not only J , the tunneling frequency, but also the parameters n , U_0 which define the interactions between the impurities. The results are too sparse to draw definite conclusions concerning the latter parameters but they do point to a $1/R^6$ interaction with a strength $U_0 \approx 30 \mu\text{K}$. This value for the HD-ortho- H_2 interaction appears surprisingly small in comparison with the strength of the interaction between ^3He impurities in solid ^4He . This can be understood qualitatively if we recall that the crystalline deformation surrounding an ortho- H_2 molecule in a para- H_2 matrix arises from the coupling between the orientation of the ortho- H_2 molecule and the lattice displacements rather than due to the blowing up the lattice due to the increase zero-point translational motion of a ^3He impurity in solid ^4He (ortho- H_2 in para- H_2 is an orientational defect while ^3He in ^4He is a mass defect). For a given ortho- H_2 orientation, the orientational crystal-field interactions are of the order of 10 mK,³⁶ and following Van Kranendonk and Sears³⁵ one expects crystalline distortional energies of the same order of magnitude; i.e., $U_0 \approx 10$ mK, and $n = 3$ in Eq. (16). Isolated molecules at relatively high temperature ($T_{\text{expt}} \geq 25$ mK) are, however, free to reorient, the reorientational rate due to thermal agitation is rapid compared to the HD tunneling frequency and the effective interaction between impurities is obtained by motional averaging due to the fast reorientations. This severely reduces the interaction seen by the HD molecules but further work is needed to understand quantitatively the value of the effective interaction implied by the experimental results. Further experimental results would also be interesting in order to confirm this tentative interpretation of the concentration dependence of the linewidth since no such clean division of the two regimes has been observed for ^3He impurities in ^4He .⁴¹

The model presented in Sec. II above for the origin of the motion responsible for the motional narrowing of the HD line shapes leads to two important predictions. Because of the mass dependence in the exponent for the expression for the tunneling frequency [$J \propto \exp(-4\sqrt{q})$ with $q \propto m$], the tunneling frequency in ortho-D₂ is much smaller than that in para-H₂ and no appreciable motional narrowing effects are expected for HD impurities in solid D₂. The HD line shapes observed in solid D₂ [$X(\text{para-D}_2) \geq 2$ at. %, $X(\text{HD}) = 0.12$ at. %, $X(\text{ortho-H}_2) = 1$ at. %]⁴² show no evidence of motional narrowing but the concentration of both ortho-H₂ and para-D₂ impurities is at the limit X_c for which the motion is quenched (for a H₂ matrix) and further experiments at much lower ortho-H₂ and para-D₂ concentrations would be valuable.

An additional test could be obtained by investigating the density dependence of the motional narrowing. The exponential factor in formula (6) for the tunneling frequency increases with increasing density largely due to the reduction in the compressibility β . ($q \propto \beta^{-1}$.) Physically, the effective potential energy δV for the tunneling determined by the compression of the surrounding molecules during the tunneling, increases as the density increases and the tunneling probability is accordingly reduced. This is the origin of the density dependence of the tunneling frequency in hcp ³He. As reported above, the frequency in hcp H₂ reduces from ~ 9 kHz at $P=0$ to ~ 100 Hz at $P=100$ bars. The motional narrowing of the HD line shapes is therefore expected to decrease rapidly for an easily accessible range of applied pressures.

A more trivial consequence of the interpretation of the NMR results in terms of a motional narrowing would be the existence of a line shift (in addition to any chemical shift) which is predicted in the case of extreme motional narrowing.^{30,43} The characteristic feature of the shift being its field dependence: maximum (~ 100 Hz) for Larmor frequencies $\nu_L \approx J$ and vanishingly small for $\nu_L \gg J$ (or $\nu_L \ll J$). While this would check the validity of the hypothesis of motional narrowing it would not offer any clues as to the origin of the motion.

A test of the motional narrowing assumption would, however, be valuable because there some questions remain concerning the relevant value of the second moment $M_{2r}(X)$ for the HD-ortho-H₂ dipolar interactions. The second moment used in the above calculations is that for interactions between HD molecules and isolated ortho-H₂ molecules. In

fact the ortho molecules migrate slowly due to their nuclear dipole-dipole interactions⁴ and eventually form pairs.^{1,44} When this clustering is completed ($\tau_c \sim \text{hour}$) the second moment is reduced by $\frac{4}{9}$ (semilike spins⁴⁵) and while this would lead one to infer smaller values of J from the experimental linewidths, a strong motional narrowing would still be needed to explain all the data.

IV. CONCLUSION

We have presented a simple model for the description of the tunneling motion in quantum solids and in particular shown that the model gives results in excellent agreement with the experimental values of the exchange frequency in hcp ³He for a wide range of molar volumes. This model predicts a tunneling frequency of the order of ~ 1 kHz for three-body cyclic permutations in hcp H₂.

Analysis of NMR line shapes of HD impurities in hcp H₂ for ortho concentrations $0.1 < X < 4$ at. % show that the data from different experimental groups can be understood quantitatively within the context of a motional narrowing model in which the nuclear dipole-dipole interactions are modulated by the tunneling motion of the HD impurities. The experimental results require a tunneling frequency $J \approx 0.6$ kHz which is in good agreement with the theoretical predictions.

The validity of the model of quantum tunneling in the solid hydrogens could be confirmed by checking two simple predictions: (a) the absence of any significant motional narrowing for HD impurities in hcp D₂ even at very low $J=1$ impurity concentrations, and (b) the density (or pressure) dependence of the tunneling frequencies in H₂ which are expected to fall in the range of 100 Hz for $P \sim 100$ bars.

ACKNOWLEDGMENTS

It is a pleasure to thank Horst Meyer, Jim Gaines, Paul Sokol, Mike Richards, Jack Hetherington, and Walter Hardy for stimulating discussions concerning the interpretation of the experimental results for solid hydrogen. André Landesman, Daniel Estève, and Michel Devoret are also warmly thanked for their many helpful criticisms. Walter Hardy is especially thanked for his critical reading of the manuscript.

¹R. Schweizer, S. Washburn, and H. Meyer, *J. Phys. (Paris)* **39**, C6-95 (1978); *Phys. Rev. Lett.* **40**, 1035 (1978).

²J. H. Constable, Ph.D. thesis (Ohio State University, 1969) (unpublished).

³J. M. Delrieu, M. Roger, and J. H. Hetherington, *J. Low Temp. Phys.* **40**, 71 (1980).

⁴R. Oyarzun and J. Van Kranendonk, *Can. J. Phys.* **50**, 149 (1972).

- ⁵J. M. Delrieu and M. Roger, *J. Phys. (Paris)* **39**, C6-123 (1978).
- ⁶M. Roger, J. M. Delrieu, and J. H. Hetherington, *J. Phys. (Paris)* **41**, C7-241 (1980).
- ⁷J. M. Delrieu, M. Roger, and J. H. Hetherington, *J. Phys. (Paris)* **41**, C7-231 (1980).
- ⁸M. Roger, Thèse de Docteur ès-Sciences (University of Paris-Sud, 1980) (unpublished).
- ⁹R. A. Guyer and L. I. Zane, *Phys. Rev.* **188**, 445 (1969); a general review of the problem of tunneling in solid ³He using a Heisenberg interaction has been given by A. Landesman, *Ann. Phys. (Paris)* **8**, 153 (1973).
- ¹⁰B. Sarkissian, Ph.D. thesis (Duke University, 1968) (unpublished).
- ¹¹A. R. Mac Mahan, *J. Low Temp. Phys.* **8**, 115, 159 (1972).
- ¹²J. P. Hansen and D. Levesque, *Phys. Rev.* **165**, 293 (1968).
- ¹³I. F. Silvera, *Rev. Mod. Phys.* **52**, 393 (1980).
- ¹⁴M. H. Kalos, D. Levesque, and L. Verlet, *Phys. Rev. A* **9**, 2178 (1974).
- ¹⁵R. A. Guyer, R. C. Richardson, and L. I. Zane, *Rev. Mod. Phys.* **43**, 532 (1971).
- ¹⁶D. J. Thouless, *Proc. Phys. Soc. London* **86**, 893 (1965).
- ¹⁷F. London, *Superfluids* (Wiley, New York, 1954), Vol. II, Sec. 56, pp. 29–31; J. S. Dugdale and J. P. Franck, *Philos. Trans. R. Soc. (London)* **257**, 1 (1965).
- ¹⁸T. Banks, C. N. Bender, and T. S. Wu, *Phys. Rev. D* **8**, 3345, 3366 (1973).
- ¹⁹A. Abramowitz and I. A. Stegun, *Handbook of Mathematical Functions* (Dover, New York, 1972).
- ²⁰G. C. Straty and E. D. Adams, *Phys. Rev.* **169**, 232 (1968).
- ²¹R. Wanner and H. Meyer, *J. Low Temp. Phys.* **11**, 715 (1973).
- ²²A. F. Andreev and I. M. Lifshitz, *Sov. Phys. JETP* **29**, 1107 (1969) [*Zh. Eksp. Teor. Fiz.* **56**, 2057 (1969)]; A. F. Andreev, *Sov. Phys. Usp.* **19**, 137 (1976) [*Usp. Fiz. Nauk* **118**, 251 (1976)].
- ²³R. A. Guyer and L. I. Zane, *Phys. Rev. Lett.* **24**, 660 (1970).
- ²⁴M. G. Richards, J. Pope, and A. Widom, *Phys. Rev. Lett.* **29**, 708 (1972); A. Widom and M. G. Richards, *Phys. Rev. A* **6**, 1196 (1972); J. E. Sacco, A. Widom, D. Locke, and M. G. Richards, *Phys. Rev. Lett.* **37**, 760 (1978).
- ²⁵M. G. Richards, J. Pope, P. S. Tofts, and J. H. Smith, *J. Low Temp. Phys.* **24**, 1 (1976).
- ²⁶A. R. Allen and M. G. Richards, *Phys. Lett.* **65A**, 36 (1978).
- ²⁷V. N. Grigoriev, B. N. Essel'son, V. A. Mikheev, V. A. Slusarev, M. A. Strzhemechny, and Yu. E. Schulman, *J. Low Temp. Phys.* **13**, 65 (1973); V. N. Grigoriev, B. N. Essel'son, and V. A. Mikheev, *Sov. Phys. JETP* **39**, 153 (1974) [*Zh. Eksp. Teor. Fiz.* **66**, 321 (1974)].
- ²⁸Y. Hirayoshi, T. Mizusaki, S. Maegawa, and H. Hirai, *J. Low Temp. Phys.* **30**, 137 (1978).
- ²⁹W. Huang, H. A. Goldberg, and R. A. Guyer, *Phys. Rev. B* **11**, 3374 (1978).
- ³⁰R. Kubo and K. Tomita, *J. Phys. Soc. Jpn.* **9**, 888 (1954).
- ³¹M. Fujio, J. Hama, and T. Nakamura, *Solid State Commun.* **13**, 1091 (1973); M. Fujio, J. Hama, and T. Nakamura, *Prog. Theor. Phys.* **54**, 293 (1975).
- ³²R. F. Buzerak, M. Chan, and H. Meyer, *J. Low Temp. Phys.* **28**, 415 (1977).
- ³³V. A. Slynsarev, M. A. Strzhemechnyi, and L. A. Burakhovich, *Sov. J. Low Temp. Phys.* **3**, 591 (1977).
- ³⁴A. B. Harris, *Phys. Rev. B* **1**, 1881 (1970).
- ³⁵S. Luryi and J. Van Kranendonk, *Can. J. Phys.* **57**, 933 (1979); J. Van Kranendonk and V. F. Sears, *Can. J. Phys.* **44**, 313 (1966).
- ³⁶R. Schweizer, S. Washburn, and H. Meyer, *J. Low Temp. Phys.* **37**, 289 (1979).
- ³⁷A. Landesman, *Phys. Lett.* **54A**, 137 (1975).
- ³⁸A. Abragam, *The Principles of Nuclear Magnetism* (Clarendon, Oxford, 1961), p. 126.
- ³⁹P. Pedroni, M. Chan, R. Schweizer, and H. Meyer, *J. Low Temp. Phys.* **19**, 537 (1975).
- ⁴⁰D. Jerome, Thèse de Docteur ès Sciences Physiques (University of Paris, 1965) (unpublished); D. Jerome, C. Ryter, and J. M. Winter, *Physics* **2**, 81 (1965).
- ^{40a}Note added in proof: Meyer and Schweizer have reanalyzed their data (Ref. 1 and unpublished results) for low ortho concentrations. Their results obtained for the transverse relaxation following a long pulse (70–100 μ s) provide additional measurements of the HD linewidth which are shown by the crosses in Fig. 5. We are grateful to these authors for communicating their results prior to publication.
- ⁴¹A. Landesman (private communication).
- ⁴²W. T. Cochran, J. R. Gaines, R. P. Mc Call, P. E. Sokol, and B. R. Patton, *Phys. Rev. Lett.* **45**, 1576 (1980).
- ⁴³A. Abragam, *The Principles of Nuclear Magnetism* (Clarendon, Oxford, 1961), p. 446.
- ⁴⁴L. I. Amstutz, J. R. Thompson, and H. Meyer, *Phys. Rev. Lett.* **21**, 1175 (1968); R. Schweizer, S. Washburn, H. Meyer, and A. B. Harris, *J. Low Temp. Phys.* **37**, 309 (1979).
- ⁴⁵We are indebted to W. N. Hardy for this observation.